Danuta Bryja
Dr hab. inż. prof. PWr
Katedra Mostów i Kolei, Wydział Budownictwa Lądowego i Wodnego,
Politechnika Wrocławska
danuta.bryja@pwr.edu.pl

Adam Popiołek
Mgr inż.
Katedra Mostów i Kolei, Wydział Budownictwa Lądowego i Wodnego,
Politechnika Wrocławska
adam.popiolek@pwr.edu.pl

DOI: 10.35117/A_ENG_18_06_03

Vibrations of the overhead catenary caused by the passage of a high-speed train through the track stiffness discontinuity

Abstract: The paper presents the methodology for simulating vibrations of the railway catenary, caused by the passage of the train through the track stiffness discontinuity. The concept of the simulation algorithm takes into account the dynamic interaction between pantographs and the overhead contact wire as well as nonlinearity resulting from the specificity of the droppers behaviour, which do not carry compression - they only carry tensile forces. The coupling of track and rail vehicles vibrations is also included. According to physics, the effect of vibrations of the catenary carried by pantographs on the railway vehicle was not taken into account, which allowed to divide the simulation algorithm into two stages and develop two computer programs with a defined hierarchy of operation. In the first stage of the simulation, the time-histories of vibrations and vibration velocities of those train cars, on which the pantographs are mounted, are calculated. In the second stage, the previously calculated time-histories are set as the input data and the vibration characteristics of the catenary and contact force between pantograph and the contact wire are calculated. The paper presents examples of vibration simulations of a rail vehicle observed in real time at the theoretical point of the pantograph base. The results of the second stage of the simulation were also shown: selected vibration time-histories of the pantograph and the five-span section of the catenary, and oscillations of the contact force between pantograph and the contact wire. The impact of the track stiffness discontinuity on catenary vibration was assessed.

Keywords: Vibration simulations; Overhead catenary; Pantographs; High-Speed train; Railway track; Track stiffness discontinuity

Introduction

In the last twenty years, many publications have appeared in the world literature devoted to the dynamics of railway traction networks. The object of many of them is to formulate and test various calculation methods designed to simulate the dynamic interaction between the pantograph and the upper traction network of the electric traction. An extensive review of this type of publication is presented, for example, in the work of the team of prof. J. Pombo [1, 12]. In the mentioned works, as well as in the work [11], a detailed description of the conditions of exploitation of traction networks and pantographs, including factors affecting the quality of power collection and the technical condition of the overhead contact line and pantograph contact strips, can be found. The dynamic interaction between the pantograph and the overhead contact line is considered to be one of the main factors and even the main factor in the case of high-speed rail. This fact justifies the great interest of scientists in the methods of simulating vibrations of traction networks, including their cooperation with pantographs. It is also reflected in the regulations, among others in standards [9, 10] and in the Commission Regulation (EU) No 1301/2014 introducing the technical specification for interoperability (TSI) of the energy subsystem [13], which component is the traction network.

According to the standard [9]: "theoretical studies of the dynamic interaction between the pantograph and the overhead contact line by means of computer simulation allow obtaining more information about the system and minimizing the costs of network research". Bearing the above in mind, the authors of simulation methods constantly improve developed algorithms, so that they better describe the real conditions of network exploitation. Despite these efforts, the influence of the kinematical exclusion of pantograph vibrations on the network vibrations has not yet been taken into account. Usually, the vertical oscillation of the pantograph base attached to the roof of the rail vehicle body is disregarded, although in reality the vehicle vibrations in the train system are recorded. The exception is the work of the team J. Ambrósio et al. [2], in which the problem of kinematic extortion has been signaled, but there is no clear calculation procedure that would examine the impact of this extortion on vibrations of the traction network. It should be emphasized that due to the effective suspension of high-speed trains, this impact is probably negligible if vehicle vibrations are forced only by slight unevenness of the running surface of the rails or by small wear of the rims. It may, however, be important in the case of incidental vibrations caused by the passage of the train due to the unevenness of the tracking threshold, especially passing at high speed.

Threshold irregularity is understood as a sudden, step change in the stiffness of the track floor, arising as a result of the discontinuity of the railway track structure or subgrade - for example, in the place of changing the bedding surface for bedding, on trips or entries to engineering structures (bridges, tunnels, culverts). Traveling the train through the threshold inequality significantly increases the dynamic impact, has an adverse effect on both the vehicle and the rail surface [3, 4, 14]. An initial statement as to whether this negative impact is also transferred to the traction network has been accepted as the practical purpose of this work. The first results of numerical research carried out using two proprietary computational programs, developed based on algorithms described by the authors in the works, will be shown [3, 4, 5, 6].

The main purpose of this work is to present the methodology of simulating vibrations of the traction network caused by the train passing through the track unevenness. The concept of the simulation algorithm takes into account the dynamic interaction between pantographs and the overhead contact line as well as non-linearity resulting from the specificity of the work of hanger cables that do not transmit compression - they only transmit tensile forces. The coupling of track vibrations and rail vehicles is also included. According to physics, the phenomenon did not take into account the influence of vibrations of traction network carried by pantographs on the railway vehicle, which allowed to divide the simulation algorithm into two stages and develop two computer programs with a fixed hierarchy. In the first stage, time courses of vibrations and vibration velocities of those train members on which the pantographs are mounted are determined. In the second stage of the simulation, the previously determined waveforms are the input data and the vibration characteristics of the traction network and the course of changes in the contact force between the pantograph and the contact wire are calculated. The paper presents examples of simulations of vibrations of a rail vehicle observed in real time at the theoretical point of mounting the pantograph base. The results of the second stage of the simulation were also shown: selected waveforms of the pantograph and the five-span section of the traction network and oscillations of the contact pressure of the pantograph on the contact wire. The impact of the threshold effect related to threshold inequalities in the railway track was assessed.

The computational model of the coupled track - train - traction network

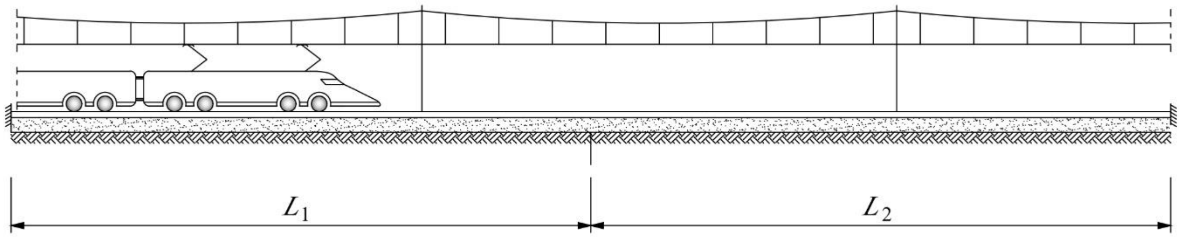

1. Scheme of the coupled track - train - traction network

In the track - train - traction network system, shown schematically in Figure **1**, two subsystems have been distinguished: (1) track - train and (2) traction network - pantographs, which are the construction element of the train. In both subsystems, there is internal feedback between the main elements, i.e. the interaction between the track and the train is mutual and interaction between the pantographs and the traction network is mutual. The physical contact point of two distinguished subsystems: (1) and (2) is the pantograph base (figures 2 and 3). It was assumed that this is a point contact - two-point if there are two pantographs in the system and one point in one pantograph. The coupling between the subsystems is called forward coupling - in the direction from the subsystem (1) to (2), i.e. the effect of vibration of the subsystem (2) on (1) is not taken into account. The calculation model of the train - train - traction network is a 2D (flat) model, targeted at the analysis of vertical vibrations of the contact wire of the traction network and analysis of the dynamic contact force between the pantograph and the contact wire.

Subsystem (1)

The dynamic model of the subsystem is shown in Fig. **2**. It was assumed that the train is an electric traction unit composed of repeating elements moving at a constant speed. Two or more pantographs are installed on the two selected train members or one. Each train member has an independent two-stage suspension and consists of a rigid body, two rigid trolleys, and four wheelsets. It is a dynamic system with 10 dynamic degrees of freedom.

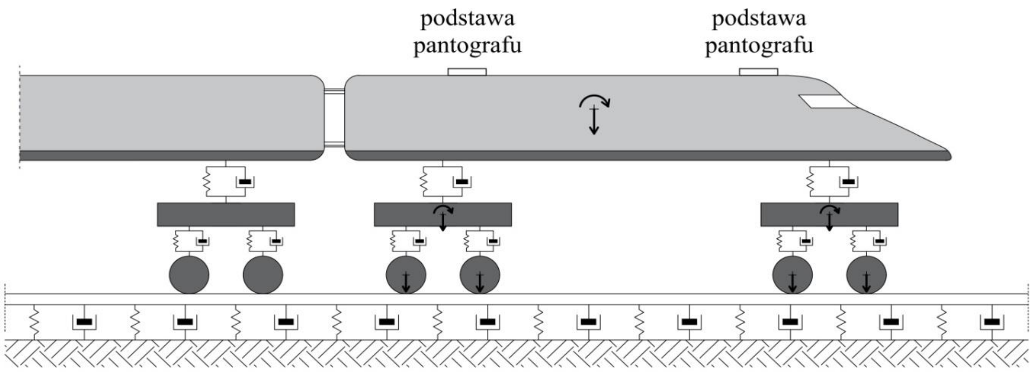

2. The dynamic model of the track - train subsystem with the indication of degrees of freedom of the rail vehicle

The railroad track is a Euler-Bernoulli-type beam resting on the Winkler's resilient ground with damping. At the border of the sections of the track L1 and L2 (see Figure **1**) there is a threshold irregularity in the form of a sudden step change in the stiffness of the elastic foundation: from the value of k1 to k2. The track with threshold irregularity is modeled using FEM in the Galerkin approach, using Euler's beam finite elements with continuous mass distribution resting on a continuous non-linear, linear visco-elastic substrate. It was assumed that the vehicle wheels remain in full contact with the rail all the time, which is a certain weakness of the model but can be relatively easily improved by introducing the Hertz-type contact bond.

Equations of motion of the coupled tor - train system were derived using the method described in detail in [3] and [4]. They are second-order differential equations with time-varying coefficients. The system of motion equations boils down to the known one in the matrix form

$$\mathbf{B}_{(1)}(t)\ddot{\mathbf{q}}_{(1)}(t) + \mathbf{C}_{(1)}(t)\dot{\mathbf{q}}_{(1)}(t) + \mathbf{K}_{(1)}(t)\mathbf{q}_{(1)}(t) = \mathbf{f}_{(1)}(t). \quad (1)$$

The solution of the system of equations (1) are the time courses of generalized coordinates $\mathbf{q}_{(1)}(t)$ and their speed $\dot{\mathbf{q}}_{(1)}(t)$ and acceleration $\ddot{\mathbf{q}}_{(1)}(t)$. The set of generalized coordinates includes deflections and rotations of path division nodes on finite elements as well as displacements and rotations of mass disks forming a dynamic train model.

Subsystem (2)

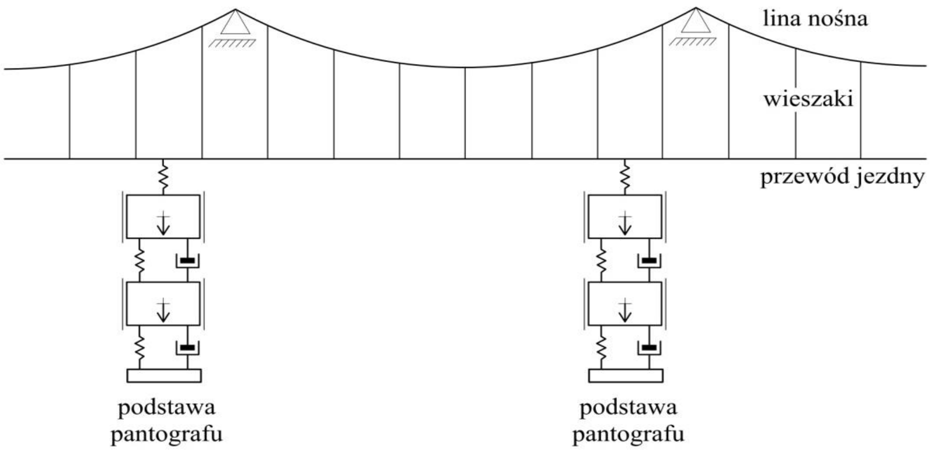

3. Model of traction network subsystem - pantographs with pantographs degrees of freedom

The adopted dynamic model of the subsystem has been schematically presented in Fig. **3**. This model is analogous to that described in detail in [5] and [6] but contains minor modifications in the definition of suspension lines and pantographs. The upper overhead contact line, similar to the initial model, is a towing hitch consisting of a multi-span carrier rope and a contact wire which is suspended to the rope by means of hangers. The supporting rope is a flaccid link supported sliding on rigid supports located at the same level. In the unloaded condition, the load-bearing rope route is parabolic within each span and the contact wire is a straight line, i.e. a string. Both of these elements are stretched by the tension forces that result from the operation of devices that tension the overhead contact line. The analyzed section of the network consists of a given number of spans, which includes one section of tensioning.

Fuzzy hangers are modeled with non-inert elastic ties that do not transmit compression, so they are ties with non-linear characteristics. Their stiffness is the same and constant, stretching k_{r}. In contrast to the initial model, suspension lines can have zero stiffness under compression, but they can also maintain a small residual stiffness characterizing the behavior of the lines during the so-called. Looseness, or loss of shape, which is equivalent to buckling. The stiffness of the compression hangers is defined by a formula $k_{\mathrm{s}} = \kappa k_{\mathrm{r}}$, where coefficient κ determines the value of residual stiffness as a small percentage of stiffness for stretching - e.g. 1%.

Adoption $\kappa = 0$ is equivalent to zero stiffness of the compression lines.

Vibrations of the cable ties with continuous mass distribution are determined by the Lagrange - Ritz approximation method, assuming that the contact wire is loaded with pantographs. Pantographs are treated as flat dynamic systems with two degrees of freedom (Figure 3), but they can be easily expanded into systems with several degrees of freedom. In contrast to the initial model described in [5] and [6], the pantograph base is not fixed, its vertical movement is determined by the vibrations of the rail vehicle at the theoretical points of contact between subsystems (1) and (2). It has been assumed, therefore, that the vertical movement of the pantograph base is described by functions $W_J^{\mathrm{p}}(t)$ i $\dot{W}_J^{\mathrm{p}}(t)$ defining the displacement and speed of vibration at the contact point J, which is also the pantograph number. These functions are determined based on the solution of the system of traffic equations (1).

After taking into account the described modifications, the equations of motion of the subsystem of the traction network - pantographs can be written in the general matrix form

$$\mathbf{B}_{(2)}\ddot{\mathbf{q}}_{(2)}(t) + \mathbf{C}_{(2)}\dot{\mathbf{q}}_{(2)}(t) + \left[\mathbf{K}_{\mathrm{const}} + \widehat{\mathbf{K}}_{\mathrm{const}} - (1-\kappa)\widehat{\mathbf{K}}_{\mathrm{ws}}(\mathbf{q}) + \widetilde{\mathbf{K}}(t)\right]_{(2)}\mathbf{q}_{(2)}(t) = \mathbf{f}_{(2)}(t) \tag{2}$$

which differs from the form of the equations given in [5]: an introduction of the coefficient κ defining the residual stiffness of hanger cables during compression and taking into account the kinematic constraint of pantographs in the excitation vector. From the point of view of taking into account the non-linear behavior of hangers, the most important is the form of stiffness matrix divided into four components. A component that changes over $\widetilde{\mathbf{K}}(t)$ results from the dynamic interaction between the overhead contact line and pantographs. The permanent component$\mathbf{K}_{\mathrm{const}}$ depends only on the elastic properties of the multi-span carrier rope and the contact wire, while the separated solid component $\widehat{\mathbf{K}}_{\mathrm{const}}$, contains all elements of the stiffness matrix dependent on the suspension lines, calculated at the initial assumption that all suspension lines have the same stiffness k_{r} both when stretched and compressed. The constituent $\widehat{\mathbf{K}}_{\mathrm{ws}}(\mathbf{q}_{(2)})$has the same structure as $\widehat{\mathbf{K}}_{\mathrm{const}}$,, but applies only to the lines identified at time t as being compressed. It is therefore dependent on generalized $\mathbf{q}_{(2)}$ coordinates defining the displacement state of the subsystem, and after subtracting from the $\widehat{\mathbf{K}}_{\mathrm{const}}$matrix taking into account the multiplier$(1-\kappa)$reduces the stiffness of compressed cables to values i $k_{\mathrm{s}} = \kappa k_{\mathrm{r}}$.

Numerical simulation method

In accordance with the adopted assumption of unilateral coupling (so-called forward coupling) of two distinguished subsystems, calculations of the influence of vibrations of the traction network carried by pantographs on the railway vehicle are not taken into account. This assumption allowed to divide the simulation algorithm into two stages and to develop two computer programs with a defined hierarchy of operation. The first program performs calculations in the subsystem (1), based on the solution of equation (1), which is determined by numerical integration using the unconditionally stable variant of the Newmark method. On the basis of this solution, vibration time courses are generated $W_J^{\mathrm{p}}(t)$ and vibration speeds$\dot{W}_J^{\mathrm{p}}(t)$ at theoretical points of interconnection of subsystems, i.e. related to those train members on which the pantographs are mounted. These waveforms constitute a subgroup of input data for the second program, which is based on the solution of equation (2) obtained also by numerical integration using the Newmark method. It is important, therefore, that the numerical integration step of both equations be the same, and, to put it more accurately, to discreetly record the course of the function $W_J^{\mathrm{p}}(t)$ i $\dot{W}_J^{\mathrm{p}}(t)$ it was consistent with the numerical integration step adopted for calculations in the second software code.

The system of motion equations (2) is quite difficult to solve because the equations are non-linear. A recursive-iterative scheme was used to solve them. At each numerical integration step, the system status was monitored by identifying hanger cables subjected to compression. Then a direct correction of the stiffness matrix was performed by subtracting the component $(1-\kappa)\widehat{\mathbf{K}}_{\mathrm{ws}}\left(\mathbf{q}_{(2)}\right)$, which reduces the effect of hanger cables in a given compression state. The correction is carried out iteratively in a given step until the accuracy of the solution vector is reached $\mathbf{q}_{(2)}$. In the first step of iteration, the correction of the stiffness matrix uses a linear solution within a given time step, based on the Newmark equation collocation equation ([8]) stored with the assumption $\kappa = 1$ (i.e. hangers are linear-elastic bonds with stiffness k_{r}).

In every step of the simulation i, on the basis of generalized displacements $\mathbf{q}_{(2)}(t_i)$ appointed at the moment t_i, the resulting quantities are calculated - contact force, lifting of the contact wire on the bracket, displacement of the pantograph head, etc. The generated time courses of the resultant result variables can be the subject of further analysis - e.g. statistical.

Input data and threshold effect simulation

A fragment of a 300 m long railway track was adopted for the tests, with the track inequalities occurring at the midpoint, thus the length of the overrun section is L_1 = 150 m. It was assumed that the stiffness of the ground on the overrun section is $k_1 = k = 1{,}1\cdot10^8$ N/m^2, on the second stretch it is fifty times bigger or smaller: $k_2 = 50k$ or $k_2 = k/50$. The ground damping parameter is fixed along the length of the track and is $2{,}8667\cdot10^5$ Ns/m^2. The flexural stiffness of the beam modeling the two rails of the railway track is $1{,}2831\cdot10^7$ Nm^2, and its unit weight $1{,}21\cdot10^2$ kg/m. The calculations included material damping in the rails with the time of retardation $2{,}1\cdot10^{-5}$ s. The vibrations of the railway track are triggered by the Shinkansen train, which consists of eight 25-meter, repeatable vehicles. Axial spacings of the carriages are shown in Fig. **4**. Mass parameters and suspension characteristics of the Shinkansen train were adopted according to the data from monograph [7]. In order to shorten the simulation time in the first tests of the simulation method presented here, the hypothetical passage of only one train member equipped with one pantograph placed in the front axle of the trolley was considered.

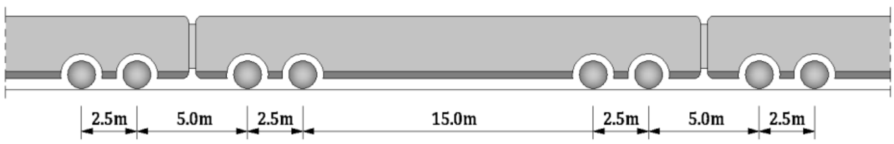

4. Axial spacing of the train bogies

Physical parameters adopted for calculations of the pantographs subsystem - traction network have been presented in table 1. They were adopted on the basis of the reference model data, which is described in the annex to the standard [9]. The length of the test section of the test network consisting of five identical spans is 300 m, i.e. it is equal to the length of the tested section of the track. Real-time simulations were carried out at two train speeds: 60 m / s and 80 m / s, taking the numerical integration time step equal to 0.001 s.

Tab. 1. Geometric and material characteristics of traction network elements and pantograph parameters

Unit weight of the lifting rope	1,07 kg/m	Pantograph speed	60 i 80 m/s
Tension of the carrying rope	16 kN	Weight of the pantographs' glider	7,2 kg
Axial stiffness of the carrying rope	12 MN	Weight of the pantograph frame	15,0 kg
Unit weight of the contact wire	1,35 kg/m	The static pressure of the pantograph	120 N
Contact wire tension	20 kN	Stiffness of the upper pantograph spring (k_1)	4 200 N/m
Stiffness of the hanger when stretched	100 kN/m	Stiffness of the lower pantograph spring (k_2)	50 N/m
The length of the span	60 m	Parameter upper pantograph silencer (c_1)	10 Ns/m
The number of spans	5	Parameter lower pantograph silencer (c_2)	90 Ns/m
Number of hangers in the span	9	Stiffness of the contact spring (k_c)	50 kN/m
Number of material damping of the carrying rope	0,5%	Number of material damping of the contact wire	0,5%

Fig. **5** shows the vertical oscillations of the pantograph base (displacement, velocity, and acceleration) generated at two train speeds (216 km / h, 288 km / h), assuming a track ground rigidity from k to 50k and from k to k / 50, which occurs after passing the 150-meter section.

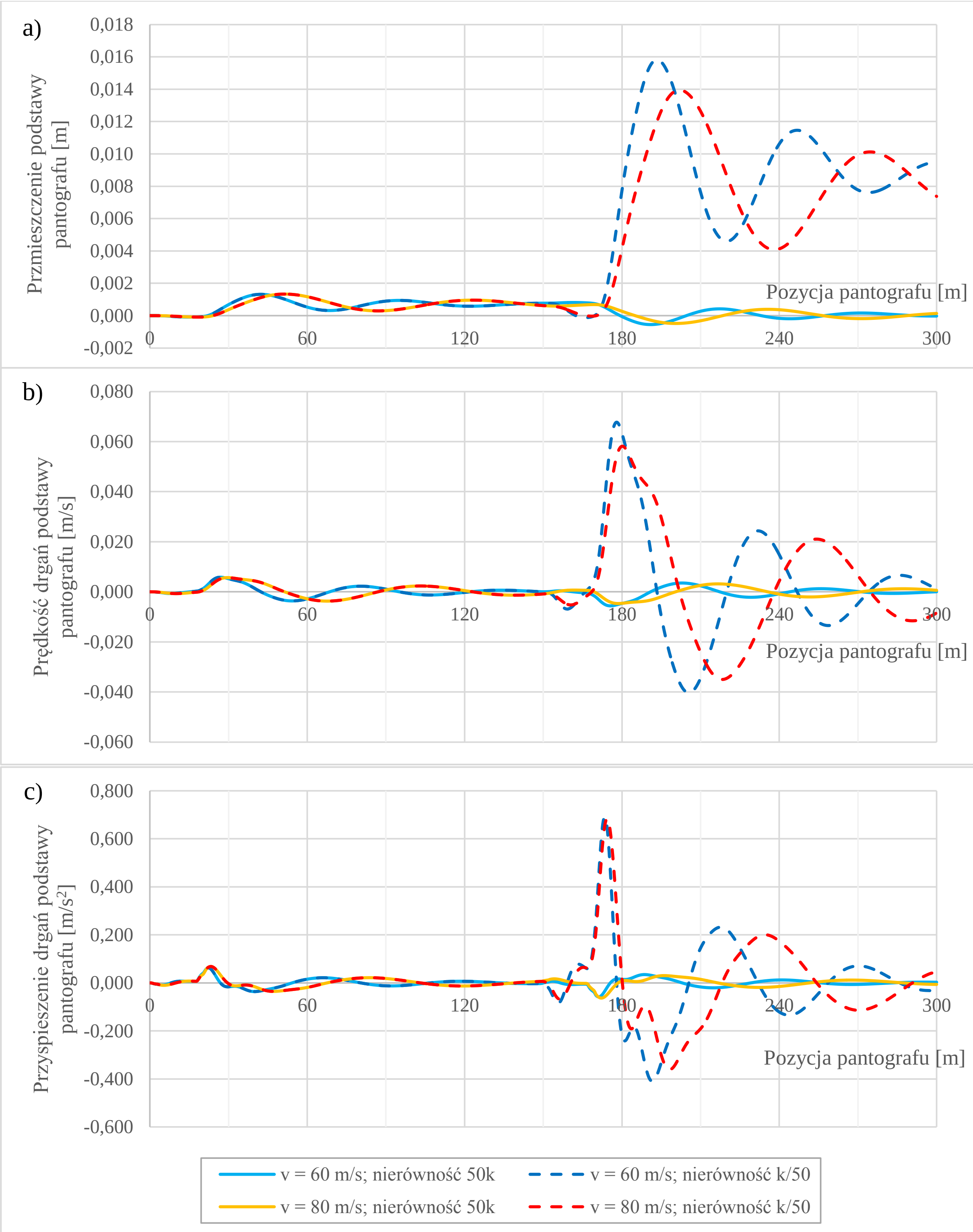

5. The vertical oscillations of the pantograph base vibrations: a) displacement, b) c) acceleration,depending on the speed of the train and the inequality of the threshold

First of all, it should be noted that in the first phase of the (overrun) vehicle movement, including the pantograph, vibrations caused by entering the vehicle onto the tested section of the track are observed, in which the rails are fixed on the left edge. The restraint results from the adopted track model - a finite length model (see Figure **1**). It can be considered that the length of the overrun section (150 m) is sufficient to obtain a fixed state of vehicle response - speed and acceleration disappear almost to zero, and the displacement is fixed at the level of constant, dynamic deflection of the rail, tracking the movement of the vehicle and its speed (compare [4]). Passing the vehicle through the threshold irregularity in the form of a fiftyfold reduction in the stiffness of the ground results in sudden excitation of vehicle vibrations, with an initial amplitude of several millimeters. Oscillating vibrations go out, aiming for a constant value - higher than the threshold inequality due to the lower stiffness of the track floor. A similar effect is observed in the case of the velocity and acceleration of vibrations, with the difference that they aim oscillating to zero. The observed dynamic threshold effect is similar to the course of the response to the impulse load. Due to the very good two-stage suspension of the vehicle body, the observed vibrations have small amplitudes, and the maximum excited accelerations affecting the driving comfort do not exceed 1 m/s2. It is worth noting that the greater threshold effect occurs at the lower of the two considered vehicle speeds, in contrast to the threshold effect occurring in rail vibrations, which evidently increases with speed ([9]). In addition, in the case of rail vibrations, the threshold effect resulting from the increase of the track bed stiffness results in large acceleration oscillations ([4]), while in the case of vehicle body vibrations (i.e., pantograph base oscillations) the impact of threshold irregularities of 50-fold increase in track stiffness is practically negligible.

It can be expected that the small vibrations of the pantograph base caused by passing through the two analyzed threshold irregularities, shown in Fig. **5**, will not have a significant impact on the vibrations of the traction network and the pantograph, which is equipped with its own vibration dampers. Fig. **6** presents the results of simulations that take into account the kinematic excitation of pantograph vibrations. As expected, the threshold effect manifests only in the vibration of the pantograph head but is negligibly small.

Summary

The highly effective suspension of the Shinkansen high-speed train rail vehicle causes that the threshold effect caused by passing through the tested threshold irregularities is so small that it practically does not transfer to the vibrations of the pantograph and the overhead contact line. Nevertheless, the calculation results shown indicate that the proposed simulation algorithm is effective and can be useful for analyzing the impact of the threshold effect on the vibrations of railway vehicles and traction networks. The main goal of the work was therefore achieved.

Further research in this area may be focused on the analysis of practical inequalities in thresholds to determine typical parameters of the track ground stiffness occurring in operational practice, and determine their impact on the vibrations of other, less efficiently sprung rail vehicles and then on vibrations of traction networks.

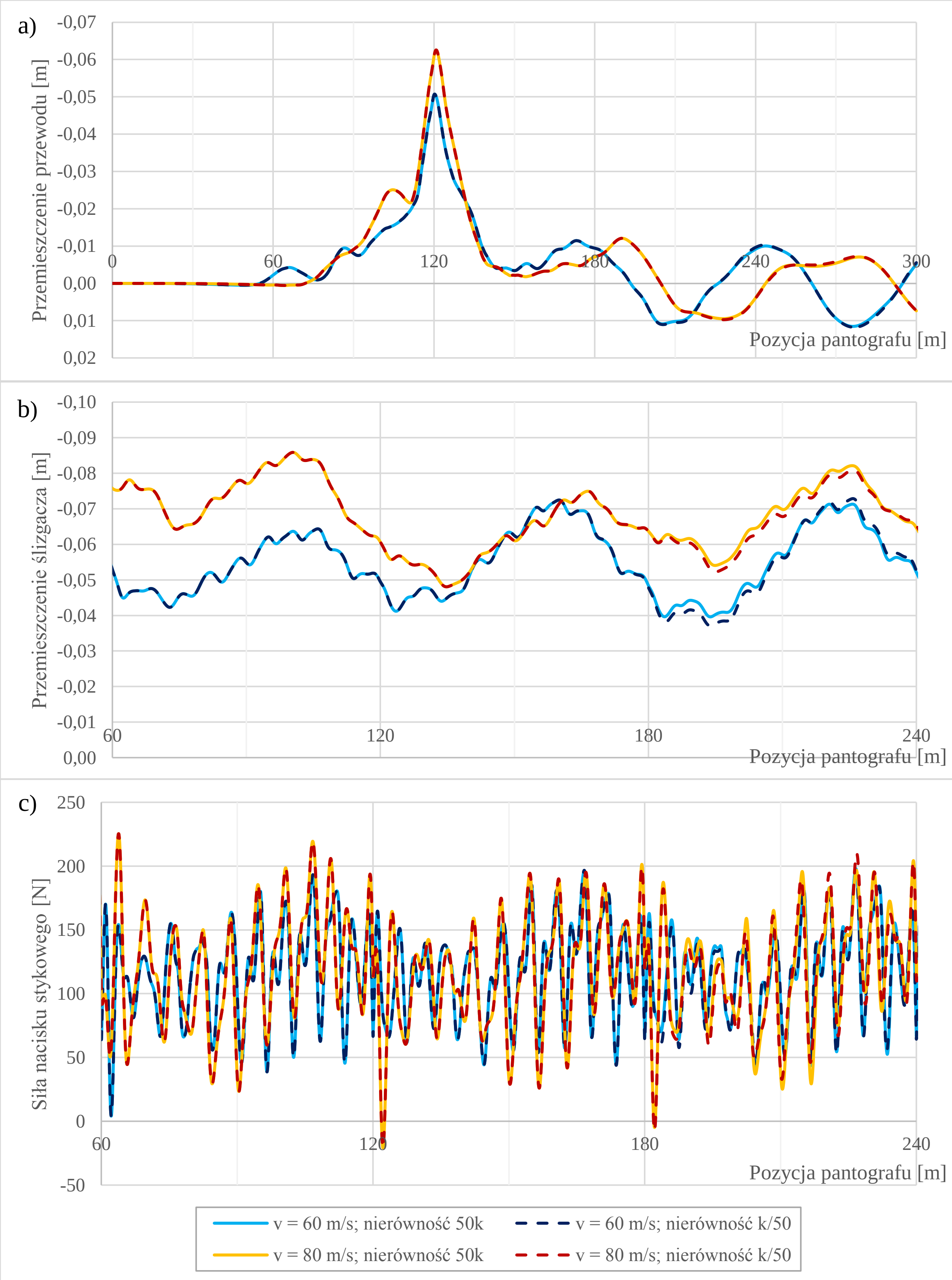

6. Timelines: a) displacement of the contact wire on the left bracket of the middle span of the test section, b) dislocation of the pantograph head, c) contact pressure, depending on the speed of the train and the threshold unevenness

Source materials

[1] Ambrósio J., Pombo J., Pereira M., Antunes P., Mósca A.: *A Computational Procedure for the Dynamic Analysis of the Catenary-Pantograph Interaction in High-Speed Trains*, Journal of Theoretical and Applied Mechanics, Vol. 50(3), 2012, pp. 681-699.

[2] Ambrósio J., Pombo J., Pereira M., Antunes P., Mósca A.: *Recent Developments in Pantograph-Catenary Interaction Modelling and Analysis*, International Journal of Railway Technology, Vol. 1(1), 2012, pp. 249-278.

[3] Bryja D., Gisterek I., Popiołek A.: *A computational method for acceleration analysis of a railway track with a stiffness discontinuity*, Proc. of the Fifteenth Int. Conf. on Civil, Structural and Environmental Engineering Computing, Prague - Czech Republic, 1-4 September 2015, ed. by J. Kruis, Y. Tsompanakis and B.H.V. Topping, Stirlingshire, Civil-Comp Press, 2015, pp. 1-13.

[4] Bryja D., Gisterek I., Popiołek A.: *Analiza numeryczna wpływu nierówności progowej na drgania toru kolejowego spowodowane przejazdem pociągu dużych prędkości*, Inżynieria i Budownictwo, r. 71, nr 10, 2015, s. 532-536.

[5] Bryja D., Popiołek A.: *Analiza drgań wieszara cięgnowego jako modelu kolejowej sieci trakcyjnej obciążonej ruchem pantografów*, Journal of Civil Engineering, Environment and Architecture, t. 34, z. 64, nr 2, 2017, s. 177-190.

[6] Bryja D.. Prokopowicz: *Dyskretno-ciągły model obliczeniowy sprzężonego układu dynamicznego: pantograf - napowietrzna sieć trakcyjna*, Przegląd Komunikacyjny, r. 71, nr 5, 2016, s. 44-51.

[7] Klasztorny M., *Dynamika mostów belkowych obciążonych pociągami szybkobieżnymi*, Wydawnictwa Naukowo-Techniczne, Warszawa 2005.

[8] Langer J.: *Dynamika budowli*, Wyd. Politechniki Wrocławskiej, Wrocław 1980.

[9] PN-EN 50318: Zastosowania kolejowe – Systemy odbioru prądu – Walidacja symulacji oddziaływania dynamicznego pomiędzy pantografem a siecią jezdną górną, PKN, Warszawa 2003.

[10] PN-EN 50367: Zastosowania kolejowe – Systemy odbioru prądu – Kryteria techniczne dotyczące wzajemnego oddziaływania między pantografem a siecią jezdną górną (w celu uzyskania wolnego dostępu), PKN, Warszawa 2012.

[11] Poetsch G., Evans J., Meisinger R., Kortüm W., Baldauf W., Veitl A., Wallaschek J.: *Pantograph/Catenary Dynamics and Control*, Vehicle System Dynamics, No. 28, 1997, pp. 159-195.

[12] Pombo J., Antunes P., Ambrósio J.: *A Study on Multiple Pantograph Operations for High-Speed Catenary Contact*, Proceedings of the Eleventh International Conference on Computational Structures Technology, B.H.V. Topping, (Editor), Civil-Comp Press, Stirlingshire, Scotland, 2012, paper 139.

[13] Rozporządzenie Komisji (UE) nr 1301/2014 z dnia 18 listopada 2014 r. w sprawie technicznych specyfikacji interoperacyjności podsystemu „Energia” systemu kolei w Unii.

[14] Sołkowski J.: *Zarys analizy efektu progowego przy łączeniu nawierzchni podsypkowych z innymi typami nawierzchni*, Technika Transportu Szynowego, r. 12, 2009, str. 59-65.